MCNN-TE: A NOVEL METHOD FOR FRACTOGRAPHIC IMAGES CLASSIFICATION BASED ON MULTI-CHANNEL CNN AND TEXTURE ENHANCEMENT

Zhen SUN[1], Junfei WU[2], Qingdang LI[3]*

Automatic classification of fractographic scanning electronic microscope (SEM) images is an important part of metal failure analysis. Using the rich texture information of SEM images, a classification method based on enhancing this information and subsequently using a multi-channel convolutional neural network (MCNN-TE) for classification is presented. Gaussian high-pass filtering is used to extract texture information, leading to texture-enhanced image sets of increasing sharpness. Through geometric transformations, the number of samples is extended and the CNNs in MCNN-TE are trained using the extended image sets. Experiments were carried out, integrating the results obtained from each channel into final classifications. Results show that the proposed method's accuracy in classifying metal fractographic SEM images reaches 96.67%. Thus, it could also be used in other industrial image texture-based classification tasks.

Keywords: Fractographic Images; Texture Enhancement; Metal Failures; Failures Classification

1. Introduction

Computer vision and pattern recognition technologies have been widely used in the field of industrial inspection, such as for defect detection in tires [1], textiles [2], and steel [3], as well as the automatic classification of industrial products [4,5]. In this paper, we discuss the application of deep learning-based image analysis [6] in metal fractographic scanning electron microscopy (SEM) images [7]. These images reflect the microscopic appearance of metal fractures and can be used to extract information about the metal fracture process [8,9]. This is a fundamental issue in the metal failure analysis process.

This issue has received some attention in recent years, with most of the studies being based on features that are not selected automatically. Minoshima, Komai and Nagasaki [10-12] presented a method for automatic classification of fractographic images based on grey-level co-occurrence matrices (GLCM),

[1] Prof., College of Electromechanical Engineering, Qingdao University of Science and Technology, China, e-mail: sunzhen@qust.edu.cn
[2] Prof., College of Electromechanical Engineering, Qingdao University of Science and Technology, China, e-mail: jfw_2002@sina.com
[3] Prof., Chinesisch-Deutsche Technische Fakultät, Qingdao University of Science and Technology, China, e-mail: lqd@qust.edu.cn

pattern recognition and cluster analysis to analyse fatigue fractures in detail. Russ [13] used a similar approach for the analysis of fractographic SEM images showing fatigue in aluminium alloys. Bastidas-Rodríguez [14,15] used fractographic images to determine fracture modes. Kosarevych [16] and Sun [17] employed histograms, Fourier power spectra, wavelet transforms and correlation vector machines for fractographic SEM image classification. Although a variety of classification methods for metal fractographic SEM images have been proposed, the accuracy of existing methods still cannot meet the practical requirements due to the complexity of the textures depicted in such images.

Therefore, in this paper, we propose a data-driven approach [18] to classify metal fractographic SEM images. This method, called MCNN-TE, first extracts texture information from the SEM images using Gaussian high-pass filtering before feeding it into a multi-channel deep convolutional neural network. The single results produced by each channel are then combined to determine the type of metal failure structure being observed according to significant texture differences between different types of metal fractographic SEM images. Experimental results indicate that the MCNN-TE can analyse the texture features contained in the images more effectively and that it outperforms previous methods with respect to accuracy.

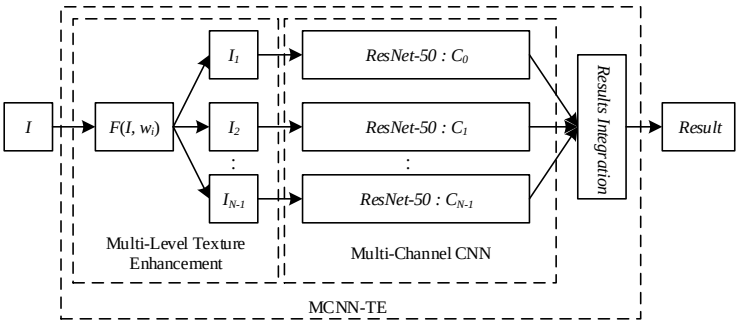

Fig. 1. MCNN-TE structure

The main contributions of our work are summarized as below:

(1) In this paper, we successfully apply a convolutional neural network to the classification of metal fractographic images through appropriate data preprocessing methods.

(2) A multi-level texture enhancement method is proposed to improve the texture of metal fracture images.

(3) The combination of multi-level texture enhancement and multi-channel convolutional neural networks has achieved good results in the classification of metal fractographic images and can provide reference for similar application scenarios.

This paper is organized into five sections. Section 2 presents basic knowledge of the metal fractographic SEM image and shows the approach of

texture enhancement and data augmentation. Section 3 presents the structure and training method of the multi-channel convolutional neural network with texture enhancement (MCNN-TE). In Section 4, we conduct some experiments to show the effectiveness of our method.

2. Material and Methods

2.1 Metal Fractographic SEM Image

Metal fractographic SEM images are collected on the fracture surfaces of various types of metal failure structures. These images are important tools for the analysis of metal failures. There are five types: dimple, cleavage, quasi-cleavage, intergranular and fatigue, as shown in Fig. 2. All images shown in this paper were obtained at the Shandong Special Equipment Inspection Institution in Jinan, China and were classified by a human expert.

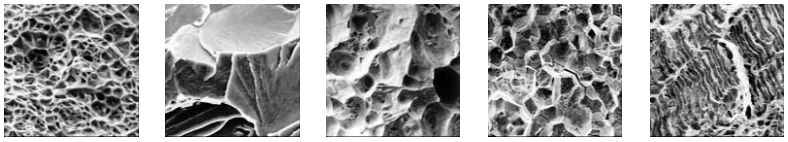

Fig. 2. Different types of metal fractographic SEM images

Different causes of metal failure can be inferred from metal fractographic SEM images as follows [7].

(1) Dimples represent a plastic fracture of the metal; the larger the dimple's size, the better the material's plasticity.

(2) Cleavages represent the occurrence of macroscopic brittle fractures, which generally occur at low temperatures, impact loads and stress concentrations.

(3) Quasi-cleavages are characteristics between cleavages and dimples, which often occur near the brittle transition temperature.

(4) Intergranular images represent the propagation of metal cracks along grain boundaries and are usually a characteristic of brittle fractures.

(5) Fatigue represents the fact that metals are subjected to alternating loads and stress concentrations. Therefore, failure analysis needs to make use of as much information as possible. In particular, quasi-cleavage, as a special morphological property between cleavage and dimple, is difficult to detect. To the best of our knowledge, there is no study on the determination of quasi-cleavage.

2.2 Enhancing Texture Information

Metal fractographic SEM images are usually greyscale images, the different types of which show different texture features. To facilitate classification, we reinforce these differences by enhancing texture information.

Let D_0 be an original image set, w a weight and F this algorithm; then $D_i = F(D_0, w)$ is the new image set with enhanced texture information. The algorithm reads as follows:

(1) For each image $I \in D_0$, perform median filtering with a filter template size of 2×4 to remove noise. The new image is represented as I_m.

(2) Apply a Fourier transform on the image.

$$I_f = \mathcal{F}(I_m) \tag{1}$$

(3) Apply high-pass filtering, where $\sigma=30$ is the cut-off frequency, and (n_1, n_2) is the centre point of I_f.

$$E_f(u,v) = H(u,v) \cdot I_f(u,v) \tag{2}$$

$$H(u,v) = 1 - e^{-\frac{(u-n_1)^2+(v-n_2)^2}{2*\sigma^2}} \tag{3}$$

(4) Perform inverse Fourier transform on the image E_f to obtain a time-domain image E containing only the texture information.

$$E = \mathcal{F}^{-1}(E_f) \tag{4}$$

(5) Perform median filtering again with template size 2×4 on the texture image E to remove tiny edges, represented as E_m.

(6) Add to the original image I the weighted texture image E_m to obtain a new image I'.

$$I' = I + E_m \cdot w \tag{5}$$

Applying the above algorithm highlights the texture features in the original image, as shown in Fig. 3. To improve legibility, we presented the images inverted.

2.3 Data Augmentation

It is well known that using convolutional neural networks [18] for image classification requires a large number of images. In the field of metal failure analysis, however, there are often few fractographic SEM images available, and small image sets will cause overfitting and reduce the recognition rate. One way to solve this problem is data augmentation. Experimental results indicate that geometric transformations on images, such as scaling, translation, rotation, or even adding noise, can be used to increase the number of images. Here, we use the ITP [19] algorithm to extend the original data, which is represented by $P(Di)$. This image transformation algorithm includes cropping, rotation, scaling, stretching, mirroring, contrast change and compression. For each iteration, a picture is randomly selected from the original image set, and one or more of the abovementioned transformation methods are randomly selected and applied to generate a new picture, as shown in Fig. 4.

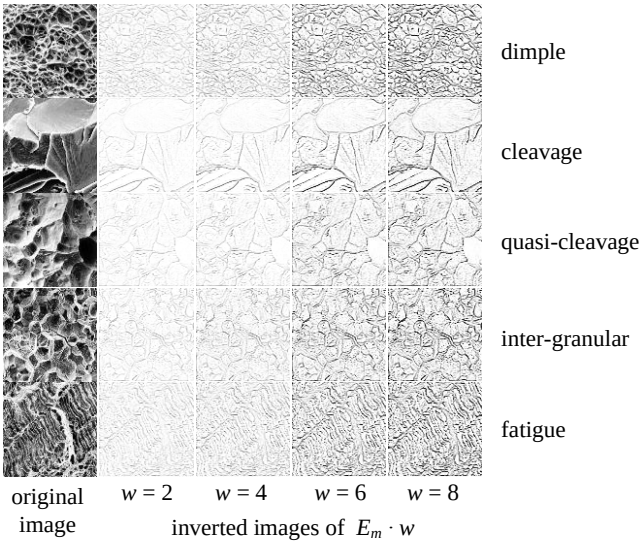

Fig. 3. Texture enhancement.

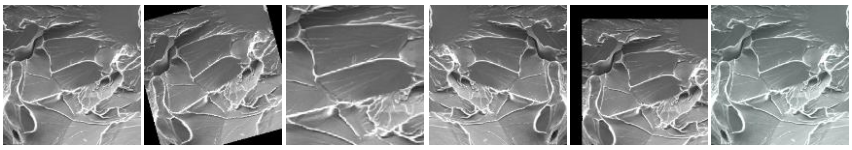

Fig. 4. Image transformation

2.4 MCNN-TE Algorithm

Expert-designed digital experiments have proven that averaging outputs of many CNNs can produce better results than only one CNN, and multi-column deep neural networks for image classification have been proposed for the classification of traffic signs [20]. Inspired by this, we propose multi-channel CNNs with texture enhancement to recognize the texture features of metal fractographic SEM images more effectively. The following two subsections describe the details of MCNN-TE.

2.5 Structure of MCNN-TE and Data Processing

The MCNN-TE method proposed in this paper utilizes N basic CNNs, C_i ($i \in [0...N\text{-}1]$), each of which has a separate training image set D_i, where D_0 is the original image set, and other training sets are obtained from D_0 by the enhancement algorithm of Section 2.2.

In the training phase, each network C_i uses the augmented image set $P(D_i)$ to improve the training effect. Through training, each basic network C_i formulates the network weights that match the characteristics of the corresponding image set. In the test phase, each test image T is extended to N images T_i ($i \in [0...N\text{-}1]$) by the

enhancement algorithm. These images are then input to the corresponding network C_i. As a result, each basic network C_i provides a probability that the test image belongs to a certain class. Finally, the average of all network outputs is taken as the MCNN-TE's final result, as shown in the following equation.

$$y_{MCNN-TE} = \frac{1}{N}\sum_{i=0}^{N-1} y_{c_i} \tag{6}$$

The training and test phases of MCNN-TE are shown in Fig. 5.

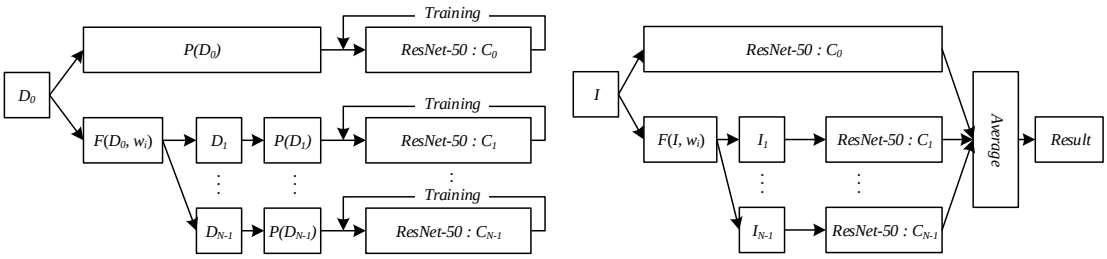

Fig. 5 MCNN-TE training phase (a) and test phase (b)

3. Results

3.1 Experiment Implementation

The experiments consist of seven steps. In the first step, the image sets are initialized, and the basic CNNs are configured. During the second step, we evaluate the effect of enhancing the texture information. The third step is determining the best parameters for texture enhancement, while in the fourth part we explore how the enhanced texture helps to increase the accuracy of classification. In the fifth phase, the optimal number of basic CNNs is determined. Finally, the accuracy achieved with the presented method is compared with state-of-the-art approaches. In addition, we analyse the misclassified samples and provide the reasons for misclassification. All of the above experiments were run on the same hardware platform, a PC with a 2.50 GHz 4-core CPU, 64 GB RAM, GeForce 1080Ti GPU with the Ubuntu 16.04 operating system and using the Matconvnet programming framework [22].

A total of 1500 fractographic SEM images of metal samples were obtained from the Special Equipment Inspection Institution. In the data initialization stage, the image resolution was uniformly set to 224×224, and histogram equalization was performed. Applying the method described in Section 3.2, the image set D_0 - D_{n-1} was generated. The test set was randomly selected out of image set D_0 with the ratio 1:4 of the test set to the training set.

The basic CNN used was a ResNet-50, to which an Fc3 layer was added to enable the recognition of the five types of metal failures. The parameter settings of each layer of the basic network are shown in Table 1. Each batch of training

sets has 30 images. The total number of iterations in the training phase was limited to 100. The learning rate was initialized to 0.01 and reduced by 10% after every 10 iterations, at which point a test with 30 images was also performed to determine whether the CNN's classification is already satisfactory.

3.2 Comparisons to the State-of-the-art

To verify the effectiveness of this method, we compared it with state-of-the-art methods. These methods can be classified into two categories.

(1) Classification algorithms based on hand-crafted features, such as kNN [23], SVM [24], KSPM [25], LLC [26], ScSPM [27].

(2) Classification algorithms based on artificial neural networks, such as BP networks [28] and ResNet-50 [21]. For the BP, kNN, and SVM algorithms, we extracted GLCM texture features from the original images as input data. For classifier selection, KSPM uses a non-linear SVM classifier, and LLC and ScSPM use a linear SVM classifier. In ResNet-50, we used the default setting and input images with data augmentation. The experimental results are shown in Table 1.

Table 1

Comparison of state-of-the-art methods

Methods	Test Accuracy (%)	Validation Accuracy (%)	Test Time (sec.)	Test Memory (MB)
BP	86.2	/	3.7	32.8
KNN	81.9	/	1.2	29.2
PCA+BP	69.44	/	3.9	36.2
ScSPM09	89.56	/	4.2	39.1
LLC10	91.85	/	4.6	42.4
KSPM-200-3	87.69	/	3.9	37.2
KSPM-400-2	88.73	/	3.7	39.3
ResNet-50	91.31	93.60	4.9	98.3
MCNN-TE	96.67	98.12	24.6	501.5

Experiments show that MCNN-TE performed best on the test sets and used the most time and memory resources. We believe that in the current hardware environment, the time and memory consumption are acceptable. Sparse coding algorithms such as ScSPM09 and LLC10 also achieved a better result. However, they require feature extraction methods and the choice of suitable classifiers, therefore their classification accuracy largely depends on the skill of the designer. The neural network-based approach avoids the uncertainty caused by expert-designed features through end-to-end training.

A few reasons for MCNN-TE's better results compared to other approaches are:

(1) The multiple convolutional and pooled layers used by the CNN extract better texture information than other methods.

(2) The enhanced texture information makes the new image set more distinguishable than the original image set.

(3) The multi-channel CNN integrates multiple results to avoid the erroneous results produced by single basic CNNs.

4. Discussion

4.1 Evaluation of the Data Augmentation

To verify the effectiveness of the ITP algorithm in the classification of metal fractographic SEM images, we conducted the following experiments: (1) Train and test a single CNN with the original image set. (2) Train a single CNN with an original image set and test with data augmentation. (3) Train a single CNN with data augmentation and test with the original image set. All experiments used the same model parameters, and the ratio of the training set, validation set and test set was 8:1:1. The results of the experiments are shown in Table 2 below.

Table 2

Effectiveness of data augmentation

No.	Training Set	Test Set	Validation Accuracy (%)	Test Accuracy (%)
1	Original Set	Original Set	91.40	89.10
2	Original Set	Augmented Set	91.40	89.02
3	Augmented Set	Augmented Set	93.60	91.31

The above experiments show that the data augmentation method reduces the overfitting of the model and improves its generalization ability. We think that there are two main reasons for this.

(1) The CNN model training process requires a large number of images. When the training image set is small, the CNN model has difficulty obtaining satisfactory test results due to insufficient parameter fitting or overfitting of parameters. The ITP method can expand a small data set to a large number of samples, providing reliable training for the CNNs.

(2) The geometric transformation method provided by ITP is well suited for metal fractographic SEM images. These images are not directional and have various scales. Different categories are mainly distinguished through the internal texture structure. The ITP method transforms the image as a whole. The new image may have a different direction, scales, etc., but the texture characteristics have not changed. Therefore, we believe that this method is effective for this paper, and the experiments also showed that using this method we can obtain better results.

4.2 Analysis of Texture Enhancement

To further explore how enhanced textures help the classification of metal

fractographic SEM images, we selected a typical cleavage image and extracted feature maps of the original image and the texture-enhanced image, as shown in Fig. 6.

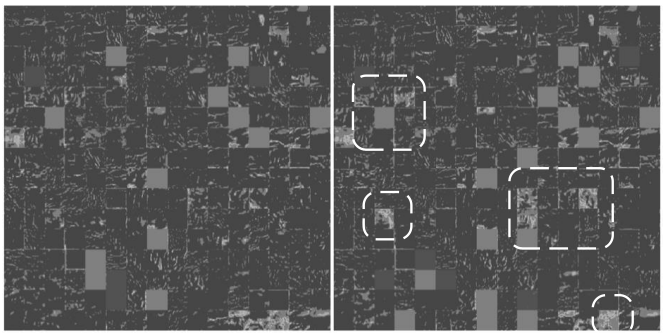

(a) (b)

Fig. 6 Feature maps of a cleavage image.
(a) Original image. (b) Texture Enhanced image with $w = 6$

By comparing the differences of the feature maps, we can see that the feature maps of the texture-enhanced images are richer, as shown in the red box. In the training phase of the CNN, these significant features are more conducive to forming the weights and the convergence of the network. In the test phase, it also helps to obtain the correct results.

4.3 Optimal Number of Basic CNNs

The MCNN-TE method may utilise one or more basic CNNs. Intuitively, more CNNs can provide more recognition capability and better accuracy, but at the same time, the computational cost of training and testing will be higher. To empirically determine the optimal number of basic CNNs, the relationship between accuracy and number of CNNs was analysed for 1, 3, 5 and 7 CNNs. The results are shown in Table 3.

Table 3

Effectiveness of data augumentation

Channel Number	Parameter *w* of each channel	Test Accuracy (%)	Validation Accuracy (%)	Training Time (sec.)	Test Time (sec.)
1	0	91.31	93.60	908.8	4.9
3	0,1,2	94.30	96.25	2728.1	14.9
5	0,1,2,4,6	96.67	98.12	4546.5	24.6
7	0,1,2,3,4,5,6	97.60	98.65	6359.2	34.5

The results show that more CNNs can provide slightly higher classification accuracy. The highest accuracy of 97.60% was achieved with 7 CNNs, followed by 96.67% with 5 and 94.30% with 3. The lowest but still acceptable accuracy of 91.31% was achieved by a single CNN (augmented image set without texture enhancement). Although more CNNs provide better accuracy,

they require considerably longer execution time and more computational resources. Because the accuracy gain from employing 5 to 7 CNNs is only marginal and does not justify the additional computational cost, we chose 5 CNNs in the MCNN-TE method.

4.4 Analysis of Misclassified Samples

The MCNN-TE had an error rate of approximately 4.2%. The recognition results for each type of fractographic SEM image are given in Table 4. The dimple images had a relatively large error rate of approximately 7.1%. Of the misclassified images, 60% were from dimple and quasi-cleavage. As mentioned in Section 2.1, quasi-cleavage is a special morphology between cleavage and dimple, and sometimes it is hard to distinguish whether an image belongs to the dimple or quasi-cleavage class. The error rate of intergranular images was also high, reaching 4.6%. Some of the samples are shown in Fig. 7.

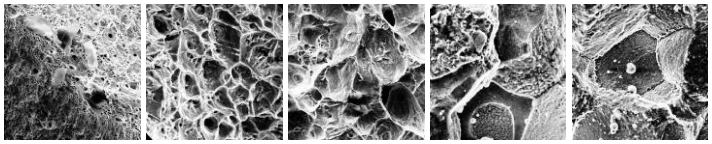

(a) (b) (c) (d) (e)

Fig. 7. Samples of misclassified images

Table 4

Recognition results

Result / Type	Dimple	Cleavage	Quasi-cleavage	Intergranular	Fatigue	Correct number	Total number	Accuracy %
Dimple	53	0	4	0	0	52	56	92.86
Cleavage	0	60	0	0	1	60	61	98.36
Quasi-cleavage	2	0	60	0	0	60	62	96.77
Intergranular	1	0	0	62	2	62	65	95.38
Fatigue	0	0	0	0	56	56	56	100
Total number						290	300	96.67

Through the analysis of these images, we found that most of them were complex textures, i.e., atypical image samples of metal fractographic SEM. Some images included several types or lied half-way between two typical classes.

5. Conclusions

Metal fractographic SEM images reflect the microscopic appearance of metal fracture and contain information about the metal fracture process. This paper presents a classification method for metal failures by enhancing texture features in fractographic images (MCNN-TE). Experiments show that the method's classification accuracy can reach 96.67%, which is superior to other

algorithms currently used in this field. This method enhances the texture and can be used in other industrial image classification tasks based on texture information.

Acknowledgements

This research was financially supported by the Tai Shan Scholar Foundation (tshw201502042), Shandong Province Key Research and Development Plan (2017CXGC0607, 2017GGX30145), National Natural Science Foundation of China (61702295).

REFERENCES

[1]. *Y. Zhang, T. Li and Q. L. Li*, "Detection of foreign bodies and bubble defects in tire radiography images based on total variation and edge detection", Chin.phys.lett, **vol.30**, no.8, 2013, pp.84205,.

[2]. *Y. Li, W. Zhao and J. Pan*, "Deformable patterned fabric defect detection with fisher Criterion-Based deep learning", IEEE Transactions on Automation Science & Engineering, **vol.14**, no.2, 2017, pp.1256-1264.

[3]. *Q. Luo and Y. He*, "A cost-effective and automatic surface defect inspection system for hot-rolled flat steel", Robotics and Computer-Integrated Manufacturing, **vol.38**, 2016, pp.16-30.

[4]. *Y. Zhang, Y. Sidibé, G. Maze, F. Leon, F. Druaux and D. Lefebvre*, "Detection of damages in underwater metal plate using acoustic inverse scattering and image processing methods", Applied Acoustics, **vol.103**, 2016, pp.110-121.

[5]. *H. Feng, Z. Jiang, F. Xie, P. Yang, J. Shi and L. Chen*, "Automatic fastener classification and defect detection in Vision-Based railway inspection systems", IEEE Transactions on Instrumentation & Measurement, **vol.63**, no.4, 2014, pp.877-888.

[6]. *M. Längkvist, L. Karlsson and A. Loutfi*, "A review of unsupervised feature learning and deep learning for time-series modeling", Pattern Recognition Letters, **vol.42**, no.1, 2014, pp.11-24.

[7]. *D. Hull*, Fractography: Observing, measuring, and interpreting fracture surface topography, Cambridge University Press, 1999.

[8]. *R. Wouters and L. Froyen*, "Scanning electron microscope fractography in failure analysis of steels", Materials Characterization, **vol.36**, no.4, 1996, pp.357-364.

[9]. *N. Adler, A. H. Dorafshar, J. P. Agarwal and L. J. Gottlieb*, "Auto-shape analysis of image textures in fractography", Image Analysis & Stereology, **vol.21**, no.2, 2011, pp.139.

[10]. *K. Komai, K. Minoshima and S. Ishii*, "Recognition of different fracture surface morphologies using computer image processing technique.", Nihon Kikai Gakkai Ronbunshu A Hen/transactions of the Japan Society of Mechanical Engineers Part A, **vol.57**, no.542, 2008, pp.2595-2601.

[11]. *K. Minoshima, T. Nagasaki and K. Komai*, "Quantitative analysis of facet sizes of cleavage failures in Sharpy impact tests using a computer image processing technique.", Nihon Kikai Gakkai Ronbunshu A Hen/transactions of the Japan Society of Mechanical Engineers Part A, **vol.54**, no.504, 2008, pp.1559-1565.

[12]. *K. Minoshima, T. Nagasaki and K. Komai*, "Automatic classification of fracture surface morphology using computer image processing technique.", Nihon Kikai Gakkai Ronbunshu A Hen/transactions of the Japan Society of Mechanical Engineers Part A, **vol.56**, no.525, 1990, pp.1318-1323.

[13]. *J. C. Russ*, Computer-assisted microscopy: The measurement and analysis of images, Springer Science & Business Media, 2012.

[14]. *M. X. Bastidasrodríguez, F. A. Prietoortíz and É. Espejomora*, "Fractographic classification in metallic materials by using 3D processing and computer vision techniques", Facultad De Ingeniería, **vol.25**, no.43, 2016, pp.83-96.

[15]. *M. X. Bastidas-Rodriguez, F. A. Prieto-Ortiz and E. Espejo*, "Fractographic classification in metallic materials by using computer vision", Engineering Failure Analysis, **vol.59**, 2016, pp.237-252.
[16]. *R. Ya. Kosarevych, O. Z. Student, L. M. Svirs'ka, B. P. Rusyn, and H. M. Nykyforchyn*, "Computer analysis of characteristic elements of fractographic images", Materials Science, **vol.48**, no.4, 2013, pp.474-481.
[17]. *Y. Sun, Z. Li and J. Yan*, "Recognition method of metal fracture images based on Wavelet kurtosis and Relevance vector machine", MATEC Web of Conferences, **vol.39**, 2016, pp.2004.
[18]. *Y. Lecun, L. Bottou, Y. Bengio and P. Haffner*, "Gradient-based learning applied to document recognition", Proceedings of the IEEE, **vol.86**, no.11, 1998, pp.2278-2324.
[19]. *J. Canny*, "A computational approach to edge detection",in Readings in Computer Vision, pp.184-203, Elsevier, 1987.
[20]. *Y. F. Pu, J. L. Zhou and X. Yuan*, "Fractional differential mask: A fractional differential-based approach for multiscale texture enhancement", IEEE Trans Image Process, **vol.19**, no.2, 2010, pp.491-511.
[21]. *A. Polesel, G. Ramponi and V. J. Mathews*, "Image enhancement via adaptive unsharp masking", IEEE Trans Image Process, **vol.9**, no.3, 2002, pp.505-510.
[22]. *M. Paulin, J. Revaud, Z. Harchaoui, F. Perronnin and C. Schmid*, "Transformation pursuit for image classification", in Proceedings of 2014 IEEE Conference on Computer Vision and Pattern Recognition, pp.3646-3653, 2014.
[23]. *D. Ciregan, U. Meier and J. Schmidhuber*, "Multi-column deep neural networks for image classification", in Proceedings of 2012 IEEE conference on Computer vision and pattern recognition (CVPR), pp.3642-3649, 2012.
[24]. *K. He, X. Zhang, S. Ren and J. Sun*, "Deep residual learning for image recognition", in IEEE Conference on Computer Vision and Pattern Recognition, pp.770-778, IEEE, 2016.
[25]. *A. Vedaldi and K. Lenc*, "Matconvnet: Convolutional neural networks for matlab", in Proceedings of the 23rd ACM international conference on Multimedia, pp.689-692, 2015.
[26]. *M. Zhang and Z. Zhou*, "ML-KNN: A lazy learning approach to multi-label learning", Pattern Recognition, **vol.40**, no.7, 2007, pp.2038-2048.
[27]. *P. H. Chen, C. J. Lin and B. Schölkopf*, "A tutorial on ν-support vector machines", Applied Stochastic Models in Business & Industry, **vol.21**, no.2, 2005, pp.111-136.
[28]. *S. Lazebnik, C. Schmid and J. Ponce*, "Beyond bags of features: Spatial pyramid matching for recognizing natural scene categories", in Proceedings of 2006 IEEE Computer Society Conference on Computer Vision and Pattern Recognition (CVPR), pp.2169-2178, 2006.
[29]. *J. Wang, J. Yang, K. Yu, F. Lv, T. Huang and Y. Gong*, "Locality-constrained linear coding for image classification", in Proceedings of 2010 IEEE Conference on Computer Vision and Pattern Recognition (CVPR), pp.3360-3367, 2010.
[30]. *J. Yang, K. Yu, Y. Gong and T. Huang*, "Linear spatial pyramid matching using sparse coding for image classification", in Proceedings of 2009 IEEE Conference on Computer Vision and Pattern Recognition (CVPR), pp.1794-1801, 2009.
[31]. *D. E. Rumelhart, G. E. Hinton and R. J. Williams*, "Learning representations by back-propagating errors", Nature, **vol.323**, no.6088, 1988, pp.399-421.